CSCE Annual Conference

Growing with youth – Croître avec les jeunes

Laval (Greater Montreal)

June 12 - 15, 2019

COMPARATIVE STUDY OF THE HEC-RAS, IBER AND FLOW 3D SOFTWARES IN STUDYING FLOW CARACTERISTICS ACROSS A DYNAMIC MEANDER IN COLOMBIA

Vargas, J.[1,3], Rivera, L.[1], Salazar, A.[1], Robledo, V.[1], Chang, P.[1], Temgoua, A. G. T.[2]
[1] Universidad Nacional de Colombia, Colombia. [2]Ottawa University, Canada.
[3] juvargasbur@unal.edu.co

Abstract: La Dorada Township (Caldas, Colombia) is located mid-way upstream along the west bank of the Magdalena River. In this region the channel banks have been affected by severe erosion as a consequence of the flow dynamics across a series of meanders. This work presents a comparative analysis of the HEC-RAS, IBER and FLOW 3D software as they are implemented in the characterization process of the channel flow dynamics, assessing their capabilities and limitations. Two field campaigns were completed in the region in February and May 2018 over the dry and rainy seasons respectively and included topographical and bathymetric surveys and river bed samples collection. Modelling of the river stretch was undertaken using a digital elevation model and field data. The three hydraulic models were prepared considering equivalent 1D, 2D and 3D conditions hence comparing simulated results among them. The study results highlighted the limitations and applicability of the 3D model in correctly modeling secondary currents across a curved channel and non-hydrostatic pressure conditions. Specifically the study points to: i) the validity of a 1D model if specific conditions related to channel characteristics and discretization of the domain can be met; ii) the shortcoming of the 2D shallow water equations in such case, and its inability to determine a non-zero, constant vertical velocity component across the channel depth; and iii) the requirement of a 3D model to correctly reproduce the three-dimensional velocity field distribution necessary to explain specific erosion processes occurring in meanders for example.

1 INTRODUCTION

The fundamental equations of hydrodynamics are based on the equations of Navier - Stokes. In general, the analysis of fluvial dynamics of a river can be undertaken by disregarding some spatial dimensions, taking into account that the scale, for example, of its length to its depth and width is significant and that the processes occurring in the vertical or horizontal dimension can be discarded within the global river analysis. In this case a number of hypotheses can be introduced to simplify the governing equations, imposing, for example, hydrostatic pressure conditions.

Generally, a longitudinal 1D model is satisfactory to correctly reproduce the processes occurring along a river (Chow, 1959). If the width of the channel is considerable and the processes occurring in this dimension are significative, a two-dimensional horizontal (2DH) model may be necessary as it allows the analysis of the transverse processes of the flow while the conditions are averaged over the channel depth (Wesseling, 2001); additionally, when the flow processes are important in other dimensions, a 3D model is required. Moreover, a full 3D model may be required in some cases where the vertical acceleration and nonhydrostatic pressure cannot be neglected. Such cases may include channel bed with abrupt changes,

short wave propagation, intensive density gradient and strong vertical circulation. (Parsapour-Moghaddam, 2017)

This study reports on the field work, modeling process and comparative analysis between the results obtained from a one-dimensional, two-dimensional and three-dimensional numerical modeling process using the HEC-RAS 5.0.5, IBER 2.4.3 and FLOW 3D 11.2 software, respectively. In this specific case, steady flow conditions were imposed to typical meandering channel way. A calibration process was not undertaken since the scope of the study was comparative.

This study was undertaken based on a previous study of the Magdalena River. As it passes though the township of La Dorada, a meandric curve is described generating severe erosion problems over the western bank of the river where the city is located. In this meander, the pressure forces are dominant at the bottom of the river and there is a flow from the outer bank in the direction of the interior part of the curve which was observed during the field campaigns. Along the channel, the flow follows the orientation of the flat curve, but it is also propelled simultaneously towards the interior/inner curve and upwards. At the same time, the flow is restricted on the outside of the curve and a helical flow (typical in a meander) is observed over the channel cross-section causing a significant lateral scour (Guarín et al., 2018).

It is known that a secondary flow is a dominant feature in meandering rivers and can impact the velocity distribution, boundary shear stress, and consequently sediment transport of the channel. Hence, it is critical to develop a model capable of reproducing flow recirculations in such cases. Moreover, given the importance of pressure gradients driving secondary flow, it is worth studying the impact of the hydrostatic pressure assumption in meander flow modelling. Considering the characteristics of a rotational flow through a meander and the geometrical characteristics of the meander itself, the three-dimensional modeling was expected to be better reproduce such flow conditions under the influence of the vertical component of the velocity vector for this type of flow (Vargas et al., 2018).

2 STUDY AREA

The study site was a 6,5km long reach of the Magdalena river near La Dorada, Colombia (5 ° 27 ' North latitude and 74 ° 40 ' East longitude). Figure 1 shows the topography of the studied area along the stretch between Motobombas and the Bridge.

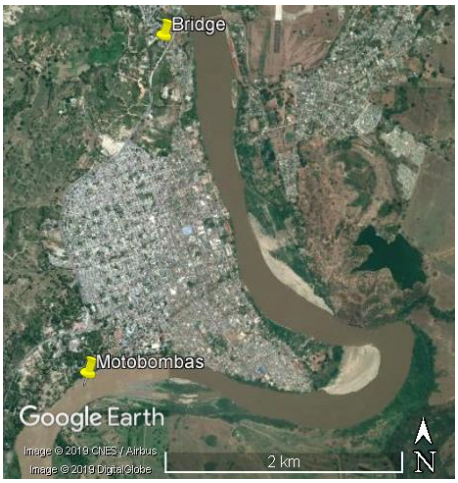

Figure 1: Study area (Google Earth, 2019)

3 FIELD SURVEY

The input data was obtained in the field evaluation developed on the 25-27 February and 6-8 May of 2018. Topographic and bathymetric surveys were carried out using a DGPS Topcon GR5 and an ADCP S5 River

Surveyor. In order to characterize the riverbed material, 31 samples were collected at the banks and the main channel. The roughness characterization was determined by the studies of Barnes (1967). The simulated events correspond to the flow rates and water levels registered by a nearby gauging station monitored by the Instituto de Hidrología, Meteorología y Estudios Ambientales (IDEAM).

4 MODELS DESCRIPTION

4.1 HEC-RAS 5.0.5 V – 1D MODEL

In a one-dimensional modeling, the channel geometry is represented as a series of cross sections (Ochoa et al., 2016). HEC-RAS is based on the energy equation proposed by Bernoulli (1738) [1] considering an incompressible and steady flow.

$$Z_2 + Y_2 + \frac{\alpha_2 V_2^2}{2g} = Z_1 + Y_1 + \frac{\alpha_1 V_1^2}{2g} + h_e \quad [1]$$

$$\alpha = \frac{\left[Q_1 V_1^2 + Q_2 V_2^2 + \ldots + Q_N V_N^2 \right]}{Q\overline{V^2}} \quad [2]$$

Where Z_1 and Z_2 are the elevations of the main channel, Y_1 and Y_2 relate to the depth of the water column, V_1 and V_2 are the average velocities, α_1 and α_2 are velocity weighting coefficients as determined by the equation [2], g is the acceleration of gravity, h_e corresponds to energy losses, Q_N and V_N are the flow rate and the velocity at each section N, respectively (USACE, 2016).

The water column of each section is determined by an iterative process solving a system of two equations [3] and [4] (Chaudhry, 2008).

$$H_2 = H_1 - h_f \quad [3]$$

$$H_2 = h_{vel} + h_{ele} \quad [4]$$

Where H_1 and H_2 are the total head at section 1 and 2 respectively, h_f relate to energy losses, h_{vel} is the velocity head and h_{ele} is the elevation head.

The energy losses between two sections are determined according to equation [5]

$$h_e = LS_f + C\left| \frac{\alpha_2 V_2^{\,2}}{2g} - \frac{\alpha_1 V_1^{\,2}}{2g} \right| \quad [5]$$

Where L stand for the weighted length, S_f represents the friction slope between two sections and C corresponds to the coefficient of expansion or contraction of the channel (USACE,2016)

4.2 IBER 2.4.3 V – 2DH MODEL

In a two-dimensional modeling, the river is discretized through a plane mesh formed by polygonal cells that model the topography of the channel. This model uses an unstructured mesh that can be formed by triangles or quadrilaterals (Bladé et al., 2012).

The IBER software is based on Saint-Venant's equations in two dimensions. In this case, hydrostatic pressure conditions and uniform vertical velocity distribution are assumed. It is also considered that the

shear over the vertical axis is negligible (Randall, 2006). Simplifications are generally valid when the vertical dimension is much smaller than any of the horizontal dimensions considered and the slope of the riverbed is negligible.

The hydrostatic pressure assumption has been widely employed in shallow water studies. From the Navier-Stokes equation, integrating the continuity equation over depth and considering the kinematic boundary conditions at bed level yields the governing Shallow Water equations (Parsapour-Moghaddam, 2017). The applicable mass conservation equations [6] and momentum conservation [7] and [8] are hence:

$$\frac{\partial h}{\partial t}+\frac{\partial hU_x}{\partial x}+\frac{\partial hU_y}{\partial y}=0 \quad [6]$$

Where h corresponds to the depth of the water sheet, U_x and U_y are the horizontal velocities averaged over depth.

$$\frac{\partial}{\partial t}\left(hU_x\right)+\frac{\partial}{\partial x}\left(hU_x^2+g\frac{h^2}{2}\right)+\frac{\partial}{\partial y}\left(hU_xU_y\right)=-gh\frac{\partial Z_b}{\partial x}+\frac{\tau_{s,x}}{\rho}-\frac{\tau_{b,x}}{\rho}+\frac{\partial}{\partial x}\left(\nu_t h\frac{\partial Ux}{\partial x}\right)+\left(\nu_t h\frac{\partial U_x}{\partial y}\right) \quad [7]$$

$$\frac{\partial}{\partial t}\left(hU_y\right)+\frac{\partial}{\partial x}\left(hU_xU_y\right)+\frac{\partial}{\partial y}\left(hU_y^2+g\frac{h^2}{2}\right)=-gh\frac{\partial Z_b}{\partial y}+\frac{\tau_{s,y}}{\rho}-\frac{\tau_{b,y}}{\rho}+\frac{\partial}{\partial y}\left(\nu_t h\frac{\partial U_y}{\partial x}\right)+\left(\nu_t h\frac{\partial U_y}{\partial y}\right) \quad [8]$$

Where g is the acceleration of gravity, Z_b is the bottom of the channel, τ_s is the surface friction due to the wind calculated though the Van Dorn equation, τ_b is the background friction calculated with Manning's equation and ν_t is the turbulent viscosity calculated using a specific model of turbulence (Bladé et al., 2012).

In this study, the turbulence model used by IBER was the $k-\varepsilon$ of Rastogi and Rodi that solves a transport equation for the turbulent kinetic energy k [9] and for the turbulent energy dissipation rate ε [10].

$$\frac{\partial k}{\partial t}+\frac{\partial U_x k}{\partial x}+\frac{\partial U_y k}{\partial y}=\frac{\partial}{\partial x_j}\left(\left(\nu+\frac{\nu_t}{\sigma_k}\right)\frac{\partial k}{\partial x_j}\right)+2\nu_t S_{ij}S_{ij}+c_k\frac{u_f^3}{h}-\varepsilon \quad [9]$$

$$\frac{\partial \varepsilon}{\partial t}+\frac{\partial U_x \varepsilon}{\partial x}+\frac{\partial U_y \varepsilon}{\partial y}=\frac{\partial}{\partial x_j}\left(\left(\nu+\frac{\nu_t}{\sigma_\varepsilon}\right)\frac{\partial \varepsilon}{\partial x_j}\right)+c_{\varepsilon 1}\frac{\varepsilon}{k}2\nu_t S_{ij}S_{ij}+c_\varepsilon\frac{u_f^4}{h^2}-c_{\varepsilon 2}\frac{\varepsilon^2}{k} \quad [10]$$

The hydrodynamic equations are solved by finite volumes conservative method which uses the integral form of the equation and considered over a segment between two consecutive mesh points (Ruiz, 2017) that define the finite volumes (Cuervo, 2012).

4.3 FLOW 3D 11.2 V – 3D MODEL

In this three-dimensional model, the geometry is discretized as cubic or rectangular elements in a structured mesh which adapts to the topography. FLOW 3D approximates the solution of the Navier – Stokes equations [11], [12], [13] and [14] using the finite difference method either implicitly or explicitly over element.

Mass conservation equation:

$$\frac{\partial uA_x}{\partial x}+R\frac{\partial vA_y}{\partial y}+\frac{\partial wA_z}{\partial z}=0 \quad [11]$$

Momentum conservation equations:

$$\frac{\partial u}{\partial t}+\frac{1}{V_F}\left\{uA_x\frac{\partial u}{\partial x}+vA_yR\frac{\partial u}{\partial y}+wA_z\frac{\partial u}{\partial z}\right\}=-\frac{1}{\rho}\frac{\partial p}{\partial x}+G_x+f_x \text{ [12]}$$

$$\frac{\partial v}{\partial t}+\frac{1}{V_F}\left\{uA_x\frac{\partial v}{\partial x}+vA_yR\frac{\partial v}{\partial y}+wA_z\frac{\partial v}{\partial z}\right\}=-\frac{1}{\rho}R\frac{\partial p}{\partial y}+G_y+f_y \text{ [13]}$$

$$\frac{\partial w}{\partial t}+\frac{1}{V_F}\left\{uA_x\frac{\partial w}{\partial x}+vA_yR\frac{\partial w}{\partial y}+wA_z\frac{\partial w}{\partial z}\right\}=-\frac{1}{\rho}\frac{\partial p}{\partial z}+G_z+f_z \text{ [14]}$$

Where V_F is the volume fraction opened to the flow, ρ is the fluid density, A_x, A_y and A_z are the opened areas to the flow in the x, y, z directions respectively, R is a coefficient which depends on the coordinate system, p is the pressure, G_x, G_y and G_z are the body accelerations, f_x, f_y and f_z are the viscous accelerations (Flow Science, 2000).

To include the turbulence effects, the Renormalized Group Model (RNG) was incorporated. This model solves two transport equations [15] and [16] in order to determine the turbulence kinetic energy and viscous dissipation independently considering a completely turbulent flow (Colman et al., 2006).

$$\frac{\partial}{\partial t}(\rho k)+\frac{\partial}{\partial x_t}(\rho kU_i)=\frac{\partial}{\partial x_j}\left[\alpha_k\mu_{eff}\frac{\partial k}{\partial x_j}\right]+G_k+G_b+\rho\varepsilon-YM+S_\kappa \text{ [15]}$$

$$\frac{\partial}{\partial t}(\rho\varepsilon)+\frac{\partial}{\partial x_t}(\rho\varepsilon U_i)=\frac{\partial}{\partial x_j}\left[\alpha_\varepsilon\mu_{eff}\frac{\partial\varepsilon}{\partial x_j}\right]+C_{1\varepsilon}\frac{\varepsilon}{k}\left(G_k+C_{3\varepsilon}G_b\right)-C_{2\varepsilon}\rho\frac{\varepsilon^2}{k}-R_\varepsilon+S_\varepsilon \text{ [16]}$$

$$\mu_{eff}=\mu\left[1+H(x)\right]^{1/3} \text{ [17]}$$

Where μ represents the viscosity, k the turbulent kinetic energy, ε the viscous dissipation, G_k the kinetic energy generation, YM the contribution due to the fluctuation of the expansion in the compressible turbulence due to the total dissipation rate, α_k and α_ε correspond to the inverse of the Prandtl number effective for κ and ε respectively, $C_{1\varepsilon}$, $C_{2\varepsilon}$ and $C_{3\varepsilon}$ are constants, S_ε and S_k are source terms, U_i represents the component of velocity in direction i, the R_ε term includes constant values obtained experimentally in order to make the model more sensitive to the effects of high deformations and curvatures of the currents lines, and *H* is a function defined between 0 and x (Ceballos, 2014).

5 NUMERICAL MODELLING

Based on the field data, a digital elevation model (DEM) of the study area was prepared (Figure 2). Also, two roughness maps were determined; one as an IBER input file with 3 Manning coefficients corresponding to the west bank, the main channel and the east bank of the river, and another as FLOW 3D input file with 3 equivalent values of d_{50}. The roughness maps spatial rendering is shown in Figure 3.

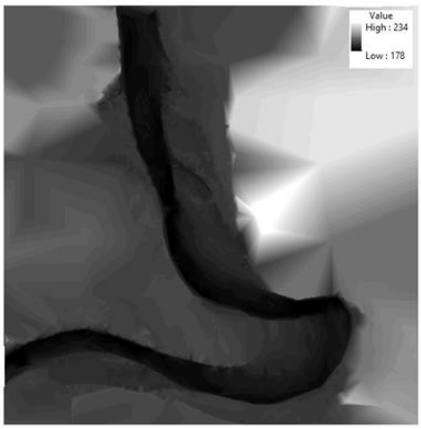

Figure 2. Digital elevation model.

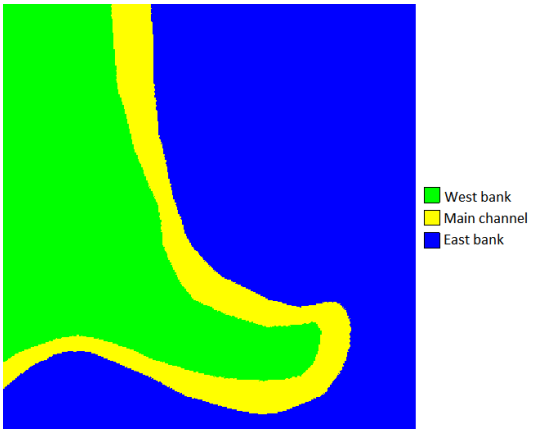

Figure 3. Roughness spatial distribution.

Table 1 presents the general characteristics of the 3 models considered in the study.

Table 1. General characteristics of the models.

CHARACTERISTIC	HEC - RAS	IBER	FLOW - 3D
GEOMETRY	• Imported as a GIS2RAS file. • Processed in ArcGIS 10.2 , extension HEC-GeoRAS.	• Imported as a ASCII file from the DEM. • Format conversion through ArcGIS 10.2.	• Imported as a ASCII file from the DEM. • Format conversion through ArcGIS 10.2.
ROUGHNESS	• Input of Manning's *n* coefficient in each section: $n_{west.} = 0.032$ $n_{channel} = 0.0125$ $n_{east} = 0.039$	• Input of Manning's *n* coefficient using a roughness map (ASCII) $n_{west.} = 0.032$ $n_{channel} = 0.0125$ $n_{east} = 0.039$	• Input of the roughness using a map of d_{50} values (ASCII) $d_{50\ west} = 0.09961$, $d_{50\ channel} = 0.00035$, $d_{50\ east} = 0.32644$. • Use of the Manning-Strickler equation to convert *n* to d_{50}.
MESH	• Sections calculated every 5 m of channel way. • Total 1416 sections along the channel.	• Unstructured mesh with triangular and square elements of 5 m on each side. • Total elements: 86927	• 4 mesh blocks with cubic cells of 5x5x5 m dimension. • Total 2560806 cells.
BOUNDARY CONDITIONS	• Flows entered as boundary condition along the initial section. • Q: 435 and 1822 m^3/s	• Flows entered in the mesh contour nodes. • Q: 435 y 1822 m^3/s	• Flows entered in the initial mesh block. • Q: 435 y 1822 m^3/s
SIMULATION TIME	-	32000 seconds. $\Delta t(s) = (0.16 – 1.0)$	13000 seconds. $\Delta t(s) = (0.02 - 0.1)$
TURBULENCE	-	$k - \varepsilon$	RNG

6 RESULTS

Figures 4-6 present the results obtained in HEC-RAS, IBER and FLOW 3D for the event simulated with a flow rate of 1822 m^3 / s as the relate to simulated channel depth.

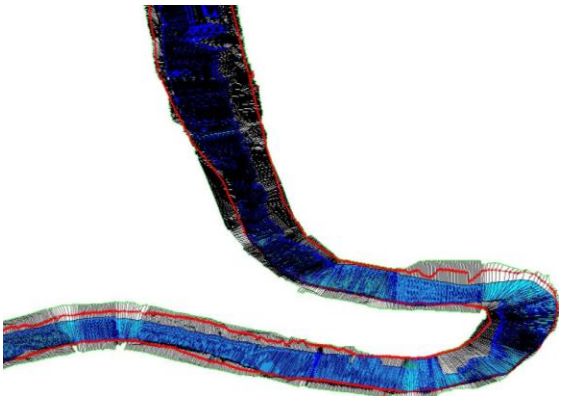

Figure 4. Depth in HEC-RAS, Q=1822 m^3/s.

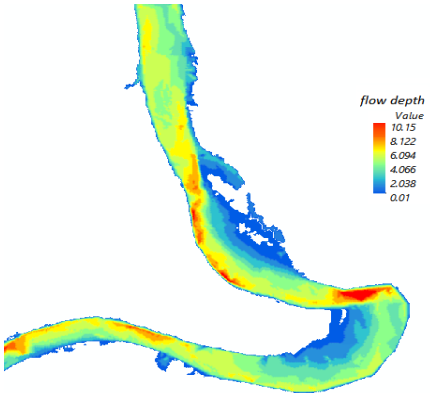

Figure 5. Depth in IBER, Q=1822 m^3/s.

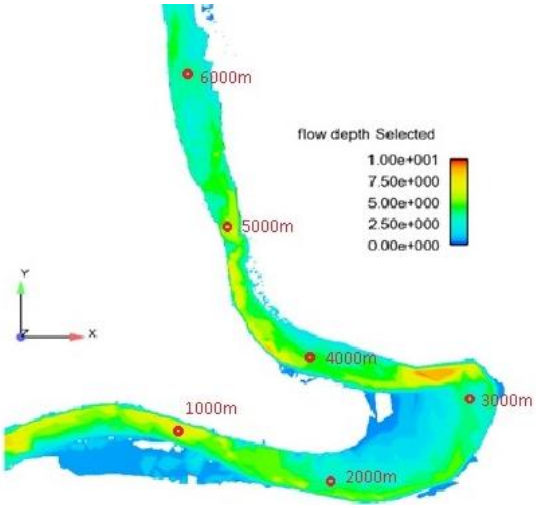

Figure 6. Depth in FLOW 3D, Q= 1822 m^3/s and longitudinal stretch of the river channel.

Figures 7 and 8 show the results of average velocity obtained in HEC-RAS, the average velocity in the depth obtained in IBER and in FLOW 3D in the main channel for a flow rate of 1822 m^3 / s and 435 m^3 / s respectively.

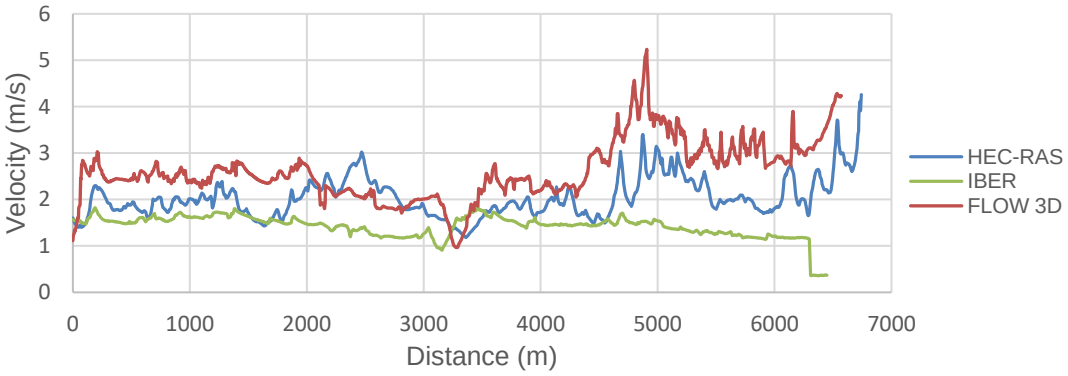

Figure 7. Comparison of simulated velocities along the channel way (Q=1822 m³/s).

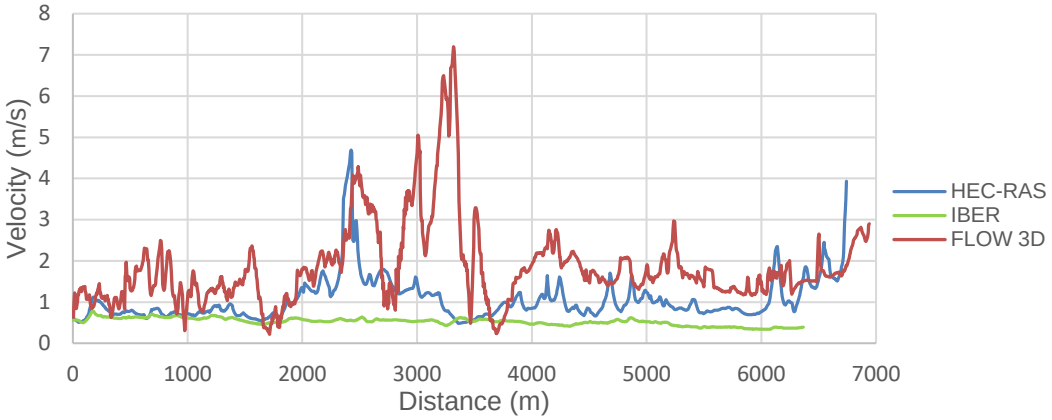

Figure 8. Comparison of simulated velocities along the channel way (Q=435 m³/s).

Figures 9 and 10 show the comparison of calculated water depth for two simulated flows.

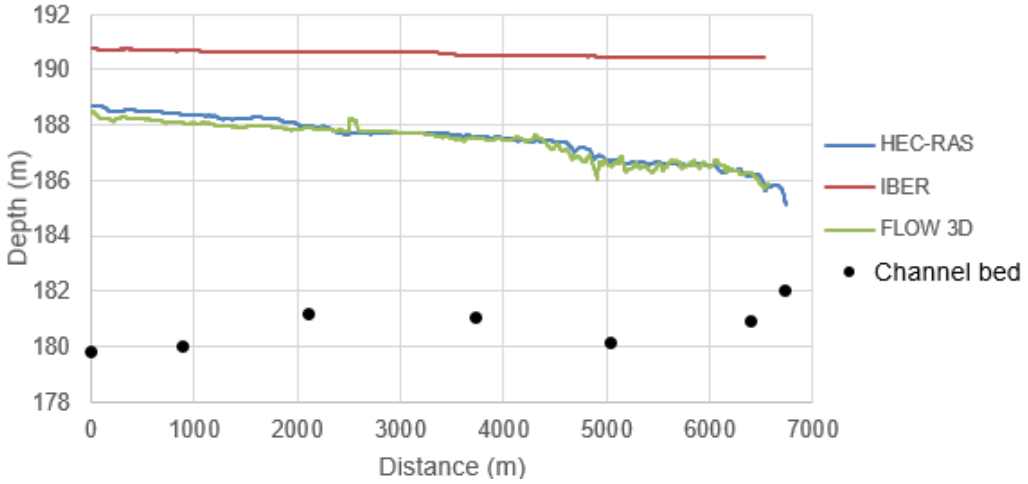

Figure 9. Comparison of simulated water levels along the channel way (Q=1822 m³/s)

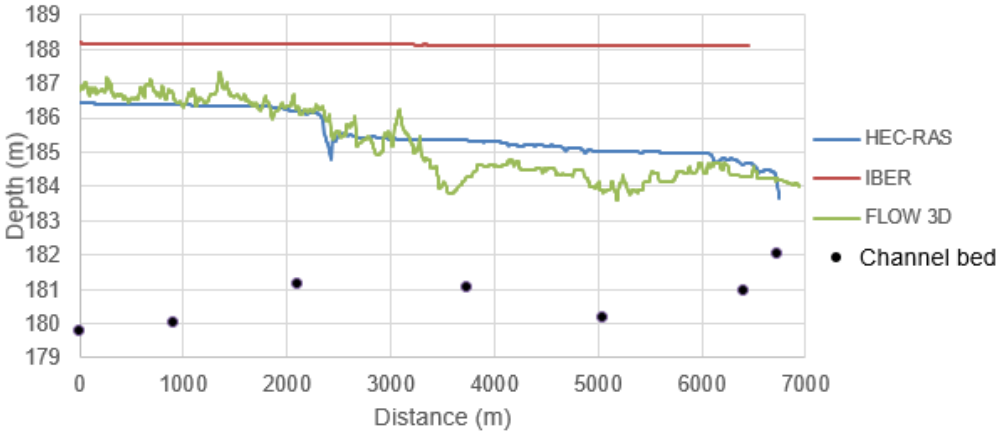

Figure 10. Comparison of simulated water levels along the channel way (Q=435 m³/s).

7 DISCUSSION

- Results obtained using HEC-RAS and FLOW 3D for the simulated events regarding the longitudinal velocity and the evolution of the water level. FLOW 3D presents higher velocities than other models. It is necessary to remember that FLOW 3D considers the three components of the velocity, therefore, the value of the resultant along the channel will tend to be higher.
- The IBER model presents a significant difference underestimating the speed along the channel and overestimating the elevation of the water level from 2 to 4 meters as compared with the FLOW 3D and HECRAS models. This velocitiy underestimation was identified in the Palavecino's study (Palavecino, 2015).
- The IBER model, based on the Boussinesq's Shallow Waters equations, has 3 underlying fundamental hypotheses: i) to satisfy the hydrostatic pressure condition, ii) to have a uniform (constant) velocity over the vertical, iii) to consider a velocity on the vertical axis that is negligible or equal to zero. Analysis of the flow through the meander revealed that none of the previous hypotheses can be verified which may explain the discrepancies obtained from the 2DH model in this case.
- The interaction mechanisms between the secondary flow and the vertical distribution of streamwise velocity plays a vital role in sharply curved bend flow modeling (Parsapour-Moghaddam, 2017), which is cleary present in this case
- The major limitation of the 1D and 2D models relate to the concealed hydrodynamic processes ocurring over the channel depth that can not be incorporated in such models.

8 CONCLUSION

The secondary flow is a transverse velocity component which is driven towards the inner bend near the riverbed and directed to the outer bend near the water surface. Due to the vertical component of this flow circulation phenomenon and the important non-hydrostatic pressure component in meander flow dynamics, it is necessary to implement a fully 3D model able to reproduce the non-linear effect between the horizontal and vertical distribution of the flow, and the non-hydrostatic pressure conditions.

The study investigated the limitations of the 1D, 2D and 3D models in hydraulic modelling of a meander using HEC RAS, IBER and FLOW 3D software respectively, and illustrated the superior performance of the FLOW 3D model regarding to the secondary flow in the studied natural meander.

The 1D model could reproduce some hydraulic variables and river characteristics. Also, it has the advantage of its simplicity and a lower computational cost . Nonetheless, the one dimensional approach cannot capture all relevant hydrodynamic processes in the specific case of a meander where occurs important processes in the horizontal and vertical dimensions.

The IBER model presents important differences with regard to the other models underestimating the speed along the channel and severally overestimating the elevation of the water column from 2 to 4 meters. Analysis of the flow through the meander revealed that none of the 2D Saint-Venant equations assumptions can be verified. In fact, it can be observed through the bathymetric survey that the bed of the channel has different longitudinal slopes, transversally changing across the section along the meander. In addition, a significant helicoidal secondary flow was observed during the field campaigns acting initially downwards from the outside bend, then across the channel width and finally upwards.

In previous studies, Lane, Bradbrook, Richards, Biron and Roy (1999) suggested that a 3D model has better predictive capability compared to a 2D model, particularly when the 2D model does not account for the effect of secondary flow (Parsapour-Moghaddam, 2017). It was found that FLOW 3D was the only model that could comprehensively reproduce 3D flow characteristics and also explain erosion processes occuring in the region.

REFERENCES

Amaya, O.D., Hernández, M.C., Silva, M.C. y Hurtado, J. (2013). *Río Magdalena: Informe Social, Económico y Ambiental*. Instituto de Estudios del Ministerio Público. Colombia.

Bladé, E., Cea, L., Corestein, G., Escolano, E., Puertas, J., Vásquez-Cendón, E., Dolz, J., y Coll, A. (2012). Iber: Herramienta de simulación numérica del flujo en ríos". *Revista Internacional de Métodos Numéricos para Cálculo y Diseño en Ingeniería*, **30**(1); 1-10.

Ceballos, A.P. (2014). *Control de flujo de acero líquido en el distribuidor mediante el diseño de la buza de la olla*. Instituto Politécnico Nacional. México D.F, México.

Chaudhry, M.H. (2008). *Open-Channel Flow*. Springer. Columbia, United States.

Colman, A., Rincón, J., Araujo, C., Materano, G. y Reyes, M. (2006). The effect of the choice of turbulence model on the simulation of fluid flow on a centrifugal separator. Influencia del modelo de turbulencia en la simulación de un separador centrífugo. *Revista Técnica de la Facultad de Ingeniería Universidad del Zulia*. Maracaibo.

Cuervo, A.E. (2012). *Comparación de los modelos hidráulicos unidimensional (HECRAS) y bidimensional (IBER) en el análisis del rompimiento de presas de materiales sueltos*. Universitat Politecnica de Catalunya. Barcelona, España.

Flow Science. (2000). *FLOW – 3D User Manual*, Release 11.2.0. FLOW – 3D. Estados Unidos.

Guarín, L.I., Vargas, J., Barreneche, S. y Chang, P. (2018). Modelling of meandering river dynamics in Colombia: A case study of the Magdalena river. *Canadian Society of Civil Engineer Annual Conference*. Fredericton, Canadá.

Julien, P.Y. (2002). *River Mechanics*. Cambridge University Press. New York, United States of America.

Ochoa, S., Reyna, T., Reyna, S., García, M., Labaque, M., y Díaz, J.M. (2016). Modelación hidrodinámica del tramo medio del río Ctalamochita, Provincia de Córdoba. *Revista Facultad de Ciencias Exactas, Físicas y Naturales*. Córdoba, Argentina.

Palavecino, A.E. (2015). *Modelación bidimensional del flujo generado por la rotura de una presa de tierra, utilizando el programa IBER*. Escuela Politécnica Nacional. Quito, Ecuador.

Parsapour-Moghaddam, P. (2017). Hydrostatic versus nonhydrostatic hydrodynamic modelling of secondary flow in a tortuously meandering river: Application of Delft3D. *Wiley Online Library. River Res Applic*. **33**: 1400-1410

Randall, D.A. (2006). *The Shallow Water Equations*. Department of Atmospheric Science. Colorado State University. Colorado, United States of America.

Ruiz, M.L. (2017). *Solución numérica de la ecuación vectorial de Saint-Venant utilizando métodos híbridos*. Universidad Michoacana de San Nicolás de Hidalgo. Michoacán, México.

Vargas, J., Guarín, L.I., y Chang, P. (2018). Modelación de la dinámica de un meandro en Colombia: Un caso de estudio en el río Magdalena. *Congreso Latinoamericano de Hidráulica*. Buenos Aires, Argentina.

Versteeg, H.K., y Malalasekera, W. (2007). *An introduction to Computational Fluid Dynamics*. Pearson Prentice Hall. Inglaterra.

US Army Corps of Engineers. (2016). *Hydraulic Reference Manual*. Hydrologic Engineering Center.